ACS APPLIED MATERIALS & INTERFACES

Research Article

www.acsami.org

Efficient Polymer Solar Cells Enabled by Low Temperature Processed Ternary Metal Oxide as Electron Transport Interlayer with Large Stoichiometry Window

Wei Lin Leong,*[,†] Yi Ren,[†] Hwee Leng Seng,[†] Zihao Huang,[†] Sing Yang Chiam,[†] and Ananth Dodabalapur[‡]

[†]Institute of Materials Research and Engineering (IMRE), Agency for Science, Technology and Research (A*STAR), 3 Research Link, Singapore 117602, Singapore

[‡]Microelectronics Research Centre, The University of Texas at Austin, Austin, Texas 78758, United States

Supporting Information

ABSTRACT: Highly efficient organic photovoltaic cells are demonstrated by incorporating low temperature solution processed indium zinc oxide (IZO) as cathode interlayers. The IZOs are synthesized using a combustion synthesis method, which enables low temperature processes (150−250 °C). We investigated the IZO films with different electron mobilities (1.4×10^{-3} to 0.23 $cm^2/(V{\cdot}s)$), hydroxide−oxide content (38% to 47%), and surface roughness (0.19−5.16 nm) by modulating the ternary metal oxide stoichiometry. The photovoltaic performance was found to be relatively insensitive to the composition ratio of In:Zn over the range of 0.8:0.2 to 0.5:0.5 despite the differences in their electrical and surface properties, achieving high power conversion efficiencies of 6.61%−7.04%. Changes in composition ratio of IZO do not lead to obvious differences in energy levels, diode parameters and morphology of the photoactive layer, as revealed by ultraviolet photoelectron spectroscopy (UPS), dark current analysis and time-of-flight secondary ion mass spectrometry (TOF-SIMS) measurements, correlating well with the large IZO stoichiometry window that enables efficient photovoltaic devices. Our results demonstrate the robustness of this ETL system and provide a convenient approach to realize a wide range of multicomponent oxides and compatible with processing on flexible plastic substrates.

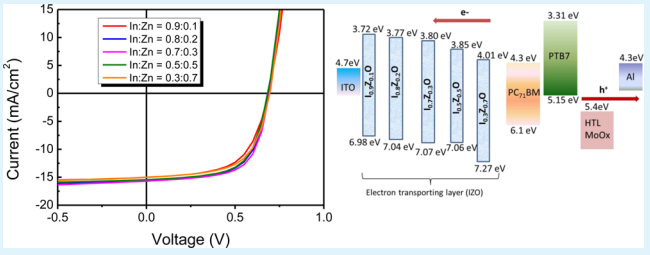

KEYWORDS: *inverted polymer solar cells, electron transporting layer, indium zinc oxide, solution process, transparent metal oxide*

INTRODUCTION

Organic and printed electronic devices such as solar cells and light-emitting diodes typically require one electrode with a work function that is sufficiently low to properly match the lowest unoccupied molecular orbital (LUMO) level of the semiconductor, for efficient injection or collection of electrons. In particular, in inverted organic solar cells, where the transparent indium tin oxide (ITO) substrate assumes the role of the cathode (electrons extracting electrode), the work function of ITO electrode needs to be modified so that there is ohmic contact to the electron transporting phase while holes are blocked (rectifying contact). Such contacts reduce interfacial recombination, improve electron extraction and lead to enhancement in short-circuit current (J_{sc}), open-circuit voltage (V_{oc}) and fill factor (FF) for higher cell efficiencies. Electron transporting layers (ETLs), which are inserted between the ITO cathode and photoactive layer, are therefore crucial for this purpose.

Among various ETLs, metal oxides such as titanium oxide or zinc oxide have been widely investigated.[1−3] These common metal oxides have many advantages including high transparency, air stability and low cost. But each type of metal oxide usually comes with a unique set of problems such as complex surface chemistries influenced by the processing conditions of the oxide.[4] The presence of defect states in the metal oxide can also serve as recombination pathways and undermine the charge blocking characteristics.[5] A common phenomenon in utilizing some of these metal oxides as electron transporting layers in organic photovoltaics is the need for "light-soaking" to improve device performance due to trap-filling in the surface defects in the metal oxide by photogenerated carriers.[4,6] In addition, pretreatment such as UV ozone or plasma of the metal oxide films is usually employed to alter the work function of the oxide in order to improve alignment with charge transport levels of the organics.[7,8] The organic photoactive layer, which is typically composed of phase separated electron-donating polymer and electron-accepting fullerene derivatives, is also highly sensitive to the surface energy of the underlying oxide layer, leading to variations in the final morphology.[9,10] Thus, the resultant solar cell performance is determined by the

Received: December 7, 2014
Accepted: May 15, 2015
Published: May 15, 2015

DOI: 10.1021/acsami.5b02215
ACS Appl. Mater. Interfaces 2015, 7, 11099−11106

underlying properties of the oxide and the minutiae associated with the surface treatment process, complicating the understanding of the influence of interfacial contact properties and creating issues of unreliability in device performance.

In thin film transistor (TFT) applications, multicomponent oxides such as zinc tin oxide (ZTO),[11,12] indium zinc oxide (IZO),[13,14] indium zinc tin oxide (IZTO)[15] and indium gallium zinc oxide (IGZO)[16−18] are found to be promising *n*-type metal oxides, with high electron mobility, small hysteresis, and good chemical and thermal stability as compared to their binary counterparts, ZnO or In_2O_3. It is therefore promising to utilize these multicomponent oxides as ETLs in solar cells, especially because a more direct route to a tunable work function can be made possible by varying the metal oxide compositions. However, such metal oxides are typically prepared using traditional vacuum deposition techniques like sputtering, chemical vapor deposition, atomic layer deposition,[6] or solution methods (e.g., sol−gel) that require postdeposition treatment under high temperatures (>400 °C) for condensation, densification and impurity removal.[19−21] The high processing temperatures involved is not compatible with roll-to-roll fabrication techniques.

In this work, we investigate the applicability of solution processed ternary metal oxides, namely, indium zinc oxide (IZO), through combustion-synthesis, as ETLs in inverted polymer solar cells. When compared to other metal oxides employed as ETLs (e.g., TiO_x and ZnO), IZO has displayed a higher electron mobility[13] and may perform the role of an ETL better. The combustion synthesis involves In and Zn precursors containing acetylacetone (fuel) and nitrate (oxidizer) that is an exothermic process. The localized energy supply can be utilized to lower the externally applied temperature for annealing of the oxide precursors.[11] But there are no reports on incorporating these combustion-synthesized IZO as ETLs in organic solar cells yet.

Herein, we demonstrate variation of the electrical (e.g., mobility, work function) and surface properties by varying the compositions in the ternary metal oxide and systematically study their effects on the photovoltaic performance. IZO with a moderate amount of Zn^{2+} is found to be advantageous when used as a cathode interlayer in inverted solar cells as they maintain a favorable energy level alignment for efficient electron extraction. The photovoltaic performance was found to be relatively insensitive to the composition ratio of In:Zn over the range of 0.8:0.2 to 0.5:0.5, achieving high power conversion efficiencies of 6.61%−7.04% in all the devices. Changes in composition ratio of IZO do not lead to obvious differences in diode parameters and morphology of the photoactive layer, which are most likely the reasons for the similarity in device performance with different IZO stoichiometries, demonstrating the robustness of this ETL system.

EXPERIMENTAL SECTION

Synthesis of IZO and Thin Film Formation. Briefly, the In and Zn precursors are prepared separately, where $In(NO_3)_3{\cdot}H_2O$ (352.2 mg) and $Zn(NO_3)_2{\cdot}6H_2O$ (297.5 mg) are dissolved in 2-methoxyethanol (5 mL), with 80.1 mg of ammonium nitrate. 0.2 mL of acetylacetone is also added into each precursor solution. After the metal salt is completely dissolved, 114 μL of 14.5 M ammonia solution is added and the solutions are aged for 48 h. The IZO solutions are finally prepared by mixing the two component solutions according to the desired molar ratios and stirred for around 1 h before film preparation. The molar ratios of In:Zn in the final precursor solutions were varied as 0.9:0.1, 0.8:0.2, 0.7:0.3, 0.5:0.5 and 0.3:0.7.

The IZO solutions are filtered through a 0.45 μm PTFE filter before spin-coating. Different IZO thin films were deposited on three different substrates, namely, quartz glass for transmittance measurements, Si/SiO_2 substrates for transistor fabrication and ITO substrates for solar cell fabrication. The IZO solutions were spin coated at 3500 rpm for 40 s. The resultant films were then annealed at 250 °C for 1 h. The thickness of these IZO films after the annealing is around 25 nm.

Characterization. The X-ray photoelectron spectroscopy (XPS) and ultraviolet photoelectron spectroscopy (UPS) measurements are performed in an ultrahigh vacuum (10^{-10} mbar) VG ESCALAB 220i-XL photoemission spectroscopy system equipped with a monochromatic Al Kα (1486.6 eV) X-ray and ultraviolet gas discharge lamp as excitation sources. The high energy resolution scans were recorded with pass energy of 20 eV and scans where applicable were carbon corrected to the binding energy of 284.6 ± 0.1 eV. The unfiltered He I (21.22 eV) photons were used for UPS work function measurements and the secondary cutoff was obtained under an applied bias of −10 V.[22] All the XPS peaks are calibrated by taking C 1s reference at 284.6 eV to compensate for any charge-induced shifts. The IZO films were inserted into the XPS chamber within 10 min after the postannealing process at 250 °C. Work function is calculated by subtracting the valence band edge to the Fermi level separation as determined from XPS, from the measured VBM (valence band edge to vacuum) as determined from UPS.

The optical properties (transmittance) were evaluated using a Shimadzu UV-3101PC UV−vis-NIR spectrophotometer. The surface morphology and roughness of the IZO films deposited on ITO substrates were studied by atomic force microscopy (Asylum Research MFP-3D stand-alone).

Time-of-flight secondary ion mass spectrometry (TOF-SIMS) depth profiling measurements were performed with a TOF-SIMS IV instrument from IONTOF GmbH using dual beam mode. A 3 keV Cs^+ ion beam was used for sputtering and a pulsed 25 keV Bi^+ was used as analysis beam with detection of negative secondary ions. Charge compensation was obtained using an electron flood gun.

Transistor Fabrication and Characterization. Heavily doped *p*-type Si and a 200 nm thick thermally grown SiO_2 layer were used as a substrate and gate oxide for the IZO TFTs, respectively. The Si/SiO_2 substrates were cleaned sequentially with deionized water, acetone and isopropyl alcohol for 10 min, followed by exposure to ultraviolet light and ozone for 30 min to produce a hydrophilic surface. The IZO solutions were spin coated at 3500 rpm for 40 s. The resultant films were then annealed at 250 °C for 1 h. A 50 nm thick aluminum (Al) thin film was deposited to complete the transistor fabrication, for source and drain electrodes through a shadow mask. The channel length and width are 100 and 4000 μm, respectively. The transistor characteristics were measured at room temperature under nitrogen with a Keithley 4200 characterization system.

Photovoltaic Device Fabrication and Characterization. The bulk heterojunction polymer/fullerene photovoltaic devices consisted of blended films of low-bandgap semiconducting polymer thieno[3,4-*b*]thiophene/benzodithiophene (PTB7; 1-materials) and [6,6]-phenyl-C_{71}-butyric acid methyl ester ($PC_{71}BM$; Solenne). All materials were used as received without further purification. PTB7:$PC_{71}BM$ blends were prepared from chlorobenzene at a weight ratio of 1:1.5. The concentration of polymer PTB7 was 10 mg/mL. A 3% v/v diiodoctane (DIO) solvent is also added into the final solution. The blend solution was stirred overnight at 70 °C in a glovebox before spin-casting.

The ITO substrates were cleaned sequentially with deionized water, acetone and isopropyl alcohol for 10 min, followed by exposure to ultraviolet light and ozone for 30 min to produce a hydrophilic surface. Inverted photovoltaic devices were made on ITO/IZO substrates by spin-casting blended films of PTB7:$PC_{70}BM$. The anode consisted of a combination of 10 nm MoO_3 (Sigma-Aldrich, 99.9%) with 80 nm of Al. The MoO_3 and Al depositions were done by thermal evaporation at a base pressure of 1.5×10^{-6} mbar. The device area was defined to be 4.5 mm^2.

Current density−voltage measurements were carried out using a Keithley 2400 source meter with an AM 1.5G solar simulator (Steuernagel, Germany model 535). The simulator lamp intensity was

DOI: 10.1021/acsami.5b02215
ACS Appl. Mater. Interfaces 2015, 7, 11099−11106

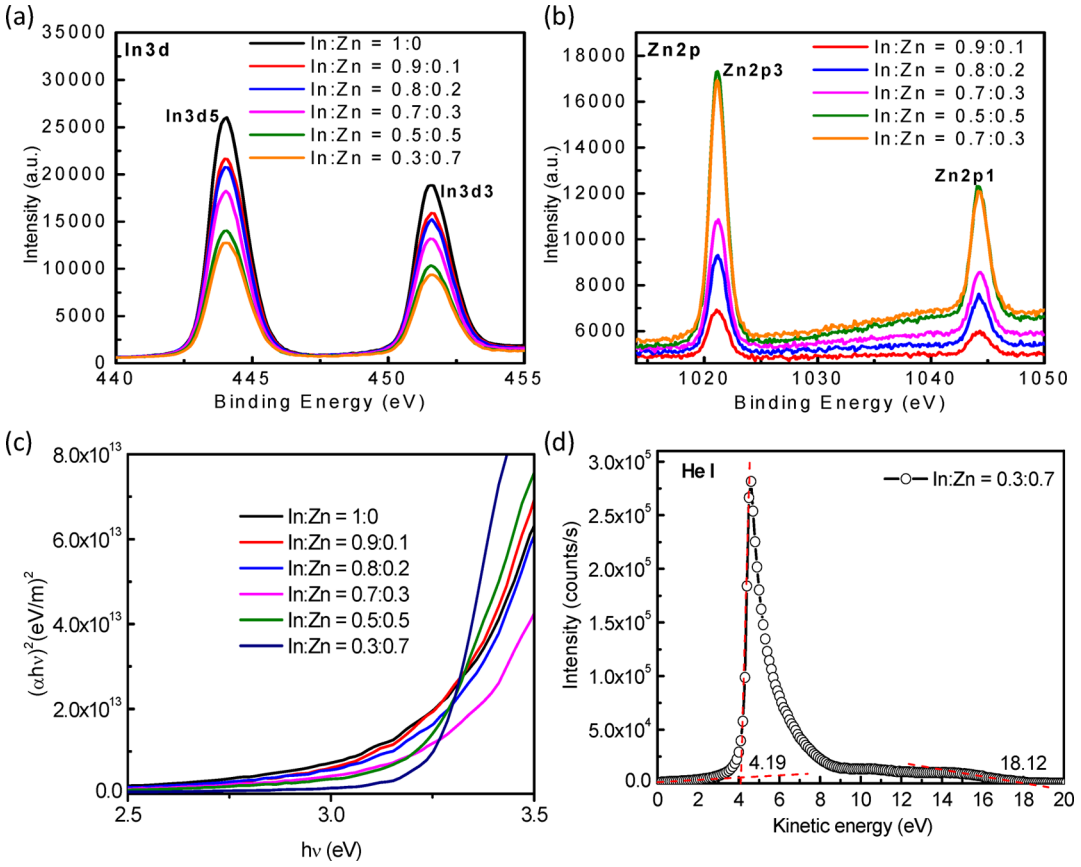

Figure 1. Corresponding narrow scans for (a) In 3d and (b) Zn 2p for In_2O_3 and IZO thin films with different molar ratios of In:Zn. (c) Tauc plots of all IZO films and (d) UPS spectrum for sample with In:Zn ratio of 0.3:0.7.

adjusted using a reference cell (Hamamatsu S1787-04) and the calculated spectral mismatch factor. Aperture masks equal to those of the Al contacts (4.5 mm^2) were used during the illuminated current−voltage measurements to accurately define the device active area. The IPCE spectra were measured using a lock-in amplifier (Stanford Research Systems, SRS 810) with white light channelled from a Newport 300 W xenon lamp and through a 212 Hz mechanical chopper wheel and a monochromator (Oriel Cornerstone 130).

RESULTS AND DISCUSSION

Physical Characteristics. The chemical composition and the electronic structure of the IZO films were studied by X-ray photoelectron spectroscopy (XPS) and ultraviolet photoelectron spectroscopy (UPS) respectively. Figure 1a,b shows the high resolution scans of the In 3d and Zn 2p core levels of the series of IZO thin films prepared at different molar ratios. The survey scans can be found in Figure S1 of the Supporting Information. All the IZO films have In $3d_{5/2}$ and Zn $2p_{3/2}$ centered at 444.1 and 1021.1 eV, indicating In−O and Zn−O bonds, respectively.[23] The In 3d and Zn 2p were monitored to estimate the relative compositions of the films. They were in line with the nominal compositions of the precursor solutions (see Table S1 of the Supporting Information), except at high Zn content (In:Zn = 0.3:0.7). The results indicate there might be limited solubility of Zn^{2+} in In_2O_3, similar to reports of tin content (Sn) in InSnO compound.[24]

The O 1s photoemission peaks presented in Figure S2 of the Supporting Information contains two peak signals. The peak centered at 529.5 eV is a characteristic lattice feature of metal−oxygen−metal (M-O-M). The feature at 531.2 eV is typically attributed to oxygen species due to formation of hydroxides, peroxides and surface species during the precursor decomposition. For the series of IZO films being investigated, one can observe a significant increase in intensity ratio between the hydroxide-to-oxide stoichiometry with increasing Zn content (Table S2 of the Supporting Information). For example, in the case of In:Zn = 0.9:0.1, the concentration of hydroxides is 40.5% whereas in the case of In:Zn = 0.5:0.5, the hydroxide concentration increases to 46.6%. These findings indicate that the hydrolysis and condensation reactions of the metal complex, which is required to form the M-O-M lattice, are mainly limited by thermal decomposition of nitrate in a zinc precursor due to stronger oxygen binding by Zn^{2+}, rather than nitrate in an indium precursor.[25] Therefore, the increasing residual impurities such as metal hydroxide in the IZO films with increasing Zn concentration can be attributed to the inefficient decomposition of a zinc precursor during the thermal annealing.

The optical band gap (E_g) was obtained from the absorption edge (Figure 1c). There is no significant change in the optical bandgap (~3.21−3.27 eV) of the IZO films with different In:Zn compositions, consistent with previous reports.[26,27] The valence band maximum (VBM) was estimated from valence band spectra in UPS measurements (Figure 1d) whereas the conduction bands of IZO can be determined by subtracting the optical bandgap from VBM. We observe an increase in conduction band level as the Zn content increased, toward the energy level of pure ZnO (4.0 eV). The energy levels of the IZO films are also summarized in Table 1. The work function of these IZO films can also be found in Table 1. There is a

DOI: 10.1021/acsami.5b02215
ACS Appl. Mater. Interfaces 2015, 7, 11099−11106

variation in the work function of 0.05−0.17 eV for the different In/Zn ratios.

Table 1. Optical Bandgaps (E_g) and Energy Levels of IZO Thin Films

	E_g	VBM (eV)	CBM (eV)	WF (eV)
In_2O_3	3.26	7.12	3.86	4.62
$In_{0.9}Zn_{0.1}O$	3.26	6.98	3.72	4.78
$In_{0.8}Zn_{0.2}O$	3.27	7.04	3.77	4.77
$In_{0.7}Zn_{0.3}O$	3.27	7.07	3.80	4.67
$In_{0.5}Zn_{0.5}O$	3.21	7.06	3.85	4.67
$In_{0.3}Zn_{0.7}O$	3.26	7.27	4.01	4.79

IZO layers spin coated on top of ITO were initially analyzed by atomic force microscopy (AFM). It is important to confirm that the combustion synthesized IZO films are uniform over the ITO electrode surface to avoid short-circuit faults when applied in inverted solar cells. The representative images are presented in Figure S3 (Supporting Information). The pristine In_2O_3 displayed a smoother amorphous morphology with root-mean-square (rms) roughness of ∼0.19 nm. For the combustion synthesized IZO films, a flat surface is generally observed, with an increase in rms roughness as the In/Zn ratios decreased (rms ∼ 0.22−5.16 nm). Note that the IZO films annealed below 400 °C typically have amorphous structures.[11,25] We have also verified the amorphous structure using X-ray diffraction (XRD), Figure S4 of the Supporting Information.

Charge Transport Properties and Conductivity. An electrical investigation of the IZO thin films was carried out using the bottom gate thin film transistor (TFT) structure described in Figure 2. IZO TFTs fabricated with different In/Zn concentrations all showed n-channel transport. For pristine In_2O_3 TFT, we observed high conductivity with no gate modulation (not shown). Figure 2a presents the transfer characteristics of IZO TFTs with different In/Zn ratios. The TFT performance parameters, including the mobility (μ), threshold voltage (V_{th}) and on/off current ($I_{on/off}$) ratio, are also summarized in Table S4 of the Supporting Information. The mobility and threshold voltage of the IZO TFTs can decrease from 0.23 to 1.4 × 10^{-3} $cm^2/(V{\cdot}s)$ and increase from 3.8 to 35.4 V respectively, as the In/Zn ratio decreases (Figure 2b). Thus, the charge transport properties of the IZO films can be tuned through appropriate control of the In/Zn ratio.

In general, In-rich composition based TFTs exhibit high off-currents, high mobilities and primarily negatively shifted threshold voltage (V_{th}) values due to the significant carrier concentrations, allowing enhanced electron conduction. In marked contrast, the Zn-rich compositions suppressed oxygen vacancy formation that reduces the free carrier generation and hence lower the off-current. This occurs because of the stronger binding of Zn−O bonds.[28] The Zn-rich compositions also contain higher hydroxides which are well-known trap sites for electrons, and the number of trap sites influences the threshold voltage. Therefore, when the number of hydroxyl groups increases, the V_{th} shifts toward a positive bias.

The bulk conductivities of the IZO films sandwiched between two electrodes were also measured. It can be seen that the currents through the IZO films of different compositions are similar, possibly due to the low film thickness (∼20−25 nm) (Figure S5 of the Supporting Information). In the subsequent sections, we demonstrate the viability of IZO thin film as ETL in photovoltaic applications and investigate the effect of change in the electrical, physical and chemical properties of the IZO films on the photovoltaic performance.

Solar Cell Performance. The inverted solar cell architecture and the energy levels of the component materials are shown in Figure 3a,b, respectively. Figure 3c presents the current density−voltage (J−V) characteristics of the devices with IZO ETLs of different In/Zn ratios. The photovoltaic parameters of these devices, as derived in Figure 3c, are also collected in Table 2. For the device using pure In_2O_3 (In:Zn = 1:0), the device shows short-circuit behavior due to high conductivity of the metal oxide film, consistent with the conductivity data (Figure S5 of the Supporting Information). The best device employs a film with In:Zn ratio of 0.7:0.3, which exhibited J_{sc} = 15.70 mA/cm^2, open-circuit voltage (V_{oc}) of 0.69 V, fill factor (FF) of 0.65 and PCE = 7.04%. The performance is also comparable to that of a conventional solar cell structure (ITO/PEDOT:PSS/PTB7:PC_{71}BM/Al), Figure S6 of the Supporting Information. Remarkably, the photovoltaic performance does not deteriorate significantly at other In/Zn ratios, with power conversion efficiencies of 6.2%−6.7%, even though the surface properties (roughness) and hydroxide−oxide content of these ETL films differ greatly. Surface properties have been reported to affect the phase segregation or morphology of the photoactive layer,[3] and presence surface trap states (due to surface groups like hydroxyl groups or oxygen adsorption) can lead to reduction in photocurrent and light-

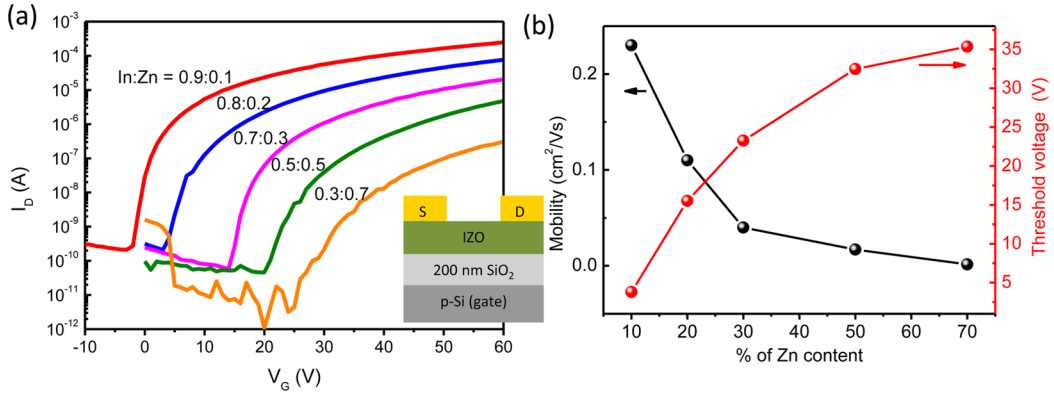

Figure 2. (a) Transfer characteristics of IZO thin film transistors with various In:Zn ratios. The channel and width are 4000 and100 μm, respectively. (b) Plot of the transistor performance parameters, including the mobility (μ), threshold voltage (V_{th}) as a function of Zn content in IZO films.

DOI: 10.1021/acsami.5b02215
ACS Appl. Mater. Interfaces 2015, 7, 11099−11106

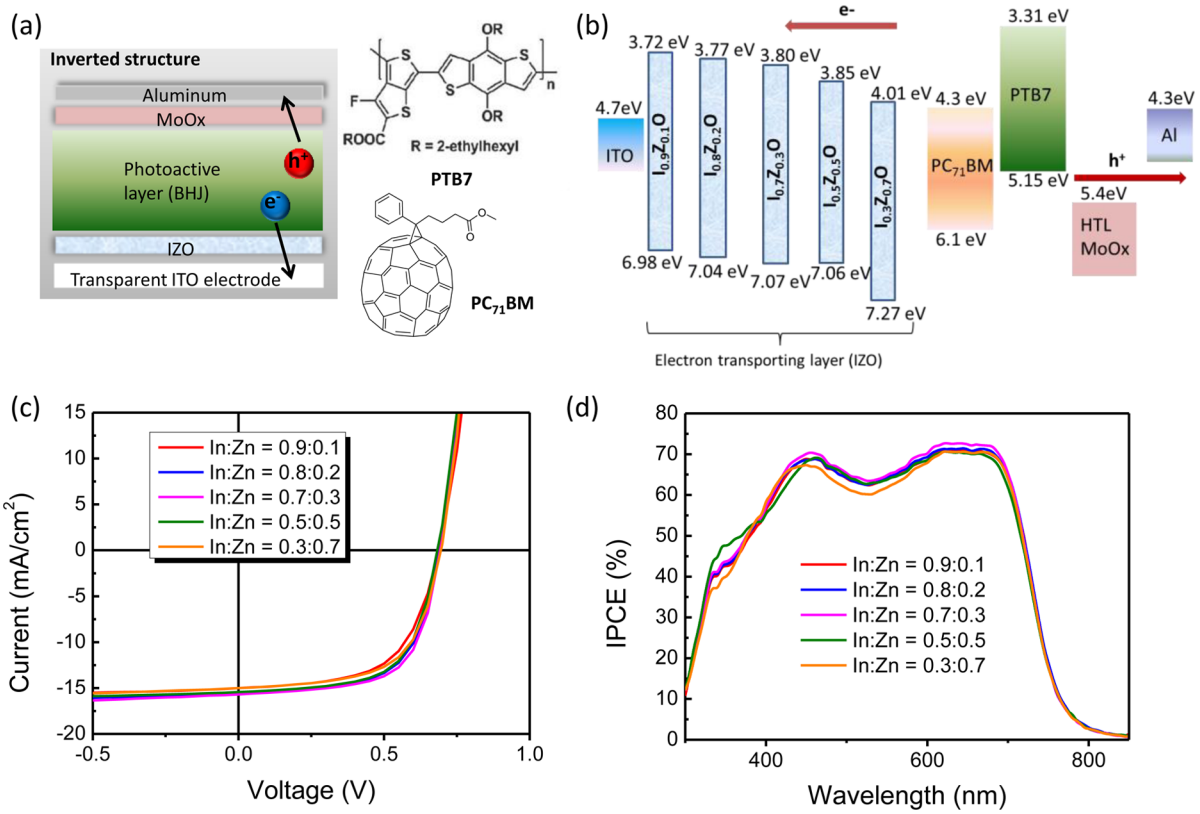

Figure 3. (a) Solar cell device schematic, (b) energy levels of the various materials used, (c) current–voltage characteristics of the solar cells incorporating different IZO as ETLs and (d) incident photon-to-current collection efficiency (IPCE) spectra of devices fabricated with the various IZO as ETLs.

Table 2. Summary of Photovoltaic Performances of PTB7:$PC_{71}BM$ Using Various Compositions of IZO as ETLs

	V_{oc} (V)	J_{sc} (mA/cm^2)	$J_{sc,\ calculated}$ (mA/cm^2)	FF	PCE (%)
$In_{0.9}Zn_{0.1}O$	0.69	15.00	15.30	0.60	6.21
$In_{0.8}Zn_{0.2}O$	0.69	15.57	15.43	0.63	6.77
$In_{0.7}Zn_{0.3}O$	0.69	15.70	15.55	0.65	7.04
$In_{0.5}Zn_{0.5}O$	0.68	15.44	15.18	0.63	6.61
$In_{0.3}Zn_{0.7}O$	0.70	15.00	15.05	0.61	6.40

soaking effect.[4,29] Our results showed that the solar cells are robust and these factors have not negatively influence the solar cell performance.

In addition, we note that there is an electron injection barrier of 0.4–0.5 eV from the LUMO of the fullerene to the CBM of IZO. But we do not observe any S-shape in the current–voltage characteristics, or light soaking effect with increasing illumination time (Figure S7a of the Supporting Information), which would otherwise indicate poor electron extraction. In addition, the J–V characteristics of the solar cells under illumination were measured without the UV spectral components and we also observe no significant change in the performance (Figure S7b of the Supporting Information). The UV spectral components were excluded through the application of an UV long-pass filter with a cutoff at 430 nm. The possible explanations are that the line-up of the IZO and $PC_{71}BM$ may involve interface dipoles,[6,30] which may substantially affect the level alignment or part of this electron barrier is compensated via spatial effects or band bending at the interface between IZO and $PC_{71}BM$.[31] Figure 3d compares the incident photon-to-current collection efficiency (IPCE) spectra of devices fabricated with the various IZO as ETLs. The IPCE of the devices exhibited similar profile shapes. High IPCE values from 500–700 nm (reaching maximum of ~73%) were observed.

We also performed the dark current analysis, and Figure 4 shows the dark current–voltages of the devices with IZO ETLs. The relevant diode parameters, including series resistance (R_s), shunt resistance (R_p), reverse saturation current density (J_o) and ideal factor, are summarized in Table S5 of the Supporting Information. There are only subtle differences in the diode parameters between the devices of different ETLs, correlating

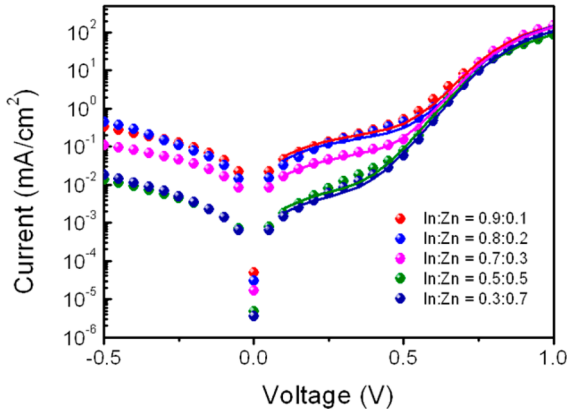

Figure 4. Dark current–voltage characteristics of solar cells using IZO with various In:Zn ratios as ETLs. The solid lines are fits to the Shockley diode equation.

DOI: 10.1021/acsami.5b02215
ACS Appl. Mater. Interfaces 2015, 7, 11099–11106

well on the large IZO stoichiometry window that enables efficient photovoltaic devices. The R_s and n for all the devices are around 1.04 to 1.97 Ωcm^2 and n = 1.79 to 1.84. The similar R_s values also corroborate with the IZO conductivity results (Figure S5 of the Supporting Information). The low R_s values suggest good contacts between active layers and cathodes, which facilitate free charge carrier extraction. There is a gradual decrease in J_o and increase in R_p as the In/Zn content decreases, indicating an enhancement in electron selectivity and reduction in charge recombination losses at the interface between the IZO and BHJ layers, possibly the reason why $In_{0.7}Zn_{0.3}O$ is the best composition as ETL and achieve high power conversion efficiency of >7%. At higher Zn content (e.g., $In_{0.3}Zn_{0.7}O$), the higher surface roughness may indicate nonuniform coverage and induce poorer contact between the IZO and photoactive layer, which in turn affects the contact resistance and fill factor.

Because the PTB7:$PC_{71}BM$ morphology can be potentially affected by the surface energy of the underlying IZO layer, the distribution of PTB7 and fullerene molecules need to be investigated. The vertical compositions of all the devices were determined by time-of-flight secondary ion mass spectrometry (TOF-SIMS). We used deuterated fullerene $PC_{61}BM$-d_5 as a substitute for $PC_{71}BM$ to establish a unique mass signal for the fullerene component.[32] Sulfur (S) and deuterium (D) signals were thus used to identify PTB7 polymer and $PC_{61}BM$-d_5, respectively. As depicted in Figure S8 of the Supporting Information, the distribution of S and D in all samples is fairly uniform throughout the organic layer, with no obvious preferential segregation of D or S phase. In all samples, slight enhancement of S profile (~10%) and corresponding lower D signal are observed in the near surface region within top 30 nm of the organic film (~150 s sputtering time). Distribution is uniform in the bulk of the organic film up to the IZO interface.

Therefore, the similarity of vertical composition of the photoactive layer on top of different stoichiometry of IZO layers, comparable diode parameters and conduction band levels (~3.77−3.85) are most likely the reasons for the invariance in V_{oc} and J_{sc}. Lastly, to demonstrate the applicability and compatibility with flexible plastic substrates, we have also lowered the processing temperature of IZO further to 150 °C, which is already sufficient to initiate the combustion reactions and has been utilized successfully as ETLs (Figure 5).

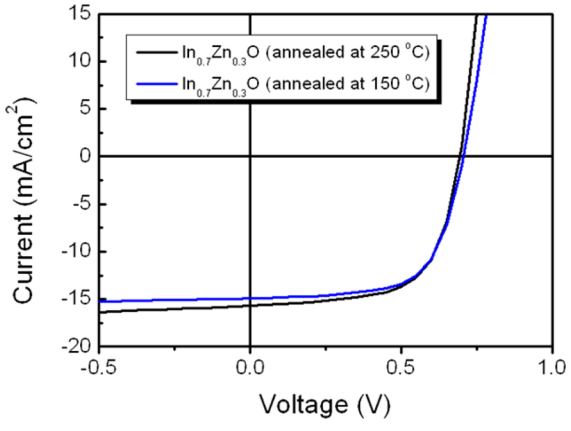

Figure 5. Current−voltage characteristics of the organic solar cells incorporating $In_{0.7}Zn_{0.3}O$ as ETLs processed at different temperatures (250 vs 150 °C).

Interestingly, the solar cell efficiency is 6.9% for $In_{0.7}Zn_{0.3}O$ film processed at 150 °C, comparable to the results obtained at 250 °C. Further efforts are in progress to lower the annealing temperature of the IZO to below 150 °C. But because the IZO films annealed at low temperature are composed primary of hydroxides, the carrier mobility and conductivity are most likely to be very low. Possible solutions are employing a deep-ultraviolet irradiation process[17] or the incorporation of gallium doping in the IZO films, which has been shown to achieve oxide-lattice structures at far lower temperatures and hence better carrier transport.[16] If the processing temperature can be lowered to below 100 °C, it can also be potentially be applicable in conventional solar cell structure where the IZO is prepared on top of the organic layers without influencing the bulk heterojunction morphology.

CONCLUSION

In this study, we demonstrated that combustion-synthesized IZO thin films fabricated at relative low temperatures function effectively as ETLs for organic solar cells. In particular, we investigated the IZO films with different electron mobilities (1.4×10^{-3} to 0.23 cm^2/(V· s)) hydroxide−oxide content (38% to 47%), and surface roughness (0.19−5.16 nm) through modulating of the stoichiometry. IZO with a moderate amount of Zn^{2+} is found to be advantageous when used as a cathode interlayer in inverted solar cells as they maintain a favorable energy level alignment for efficient electron extraction. Remarkably, a large window of IZO stoichiometry (In:Zn = 0.8:0.2 to 0.5:0.5) was established for the devices incorporating IZO as the ETL, achieving high power conversion efficiencies of 6.61%−7.04%. We observe comparable diode parameters (R_s, n, J_o, R_p) and invariant in the vertical composition of the photoactive layer with different stoichiometries of the IZO films, which are the main reasons for the close similarity in device performance, demonstrating the robustness of this ETL system. Our results provide a convenient approach to realize IZO ETLs through the combustion synthesis method, which allow us to use low processing temperatures (150−250 °C) and hence compatible with processing on flexible plastic substrates. This work can also inspire other multicomponent oxides through the combustion synthesis method for photovoltaic applications.

ASSOCIATED CONTENT

Supporting Information

Survey scan for In_2O_3 and IZO thin films with different molar ratios of In:Zn, composition of precursor solutions and relative composition of resultant IZO films, XPS spectra showing M-O-M lattice oxygen and M-OH metal hydroxide oxygen, concentration of hydroxides in the IZO films, atomic force microscopy images of the combustion synthesized IZO films on ITO substrates, table summary of surface roughness of the IZO films and device parameters of IZO thin film transistors, typical X-ray diffraction (XRD) of combustion synthesized IZO (In:Zn = 0.7:0.3) at annealing temperature of 250 °C, current−voltage characteristics for IZO films on ITO substrate and top Al electrode, current−voltage characteristics of the organic solar cells in conventional structure; ITO/PEDOT:PSS/PTB7:$PC_{71}BM$/Al, fit parameters for the dark J−V curves of PTB7:$PC_{71}BM$ using IZO as ETLs, J−V characteristics of inverted solar cells based on IZO ETL (with In:Zn = 0.5:0.5) with different illumination time, J−V characteristics of inverted solar cells based on IZO ETL (with In:Zn = 0.7:0.3) under

DOI: 10.1021/acsami.5b02215
ACS Appl. Mater. Interfaces 2015, 7, 11099−11106

illumination, with and without the UV filter, as well as time-of-flight secondary ion mass spectrometry (TOF-SIMS) plots for PTB7:$PC_{61}BM$-d_5 blend films. The Supporting Information is available free of charge on the ACS Publications website at DOI: 10.1021/acsami.5b02215.

AUTHOR INFORMATION

Corresponding Author

*W. L. Leong. E-mail: leongwl@imre.a-star.edu.sg.

Notes

The authors declare no competing financial interest.

ACKNOWLEDGMENTS

The authors thank A*STAR IMRE Molecular Materials Project (IMRE/13-1P0909) for funding support. W. L. Leong thanks Mr. Rajiv Ramanujam Prabhakar and Mr. Rohit Abraham John for help in the AFM and XRD measurements.

REFERENCES

(1) Zilberberg, K.; Meyer, J.; Riedl, T. Solution Processed Metal-Oxides for Organic Electronic Devices. *J. Mater. Chem. C* **2013**, *1*, 4796−4815.

(2) Yip, H. L.; Jen, A. K. Y. Recent Advances in Solution-Processed Interfacial Materials for Efficient and Stable Polymer Solar Cells. *Energy Environ. Sci.* **2012**, *5*, 5994−6011.

(3) Chen, L. M.; Xu, Z.; Hong, Z.; Yang, Y. Interface Investigation and Engineering - Achieving High Performance Polymer Photovoltaic Devices. *J. Mater. Chem.* **2010**, *20*, 2575−2598.

(4) Bok Kim, J.; Ahn, S.; Ju Kang, S.; Nuckolls, C.; Loo, Y. L. Ligand Chemistry of Titania Precursor Affects Transient Photovoltaic Behavior in Inverted Organic Solar Cells. *Appl. Phys. Lett.* **2013**, *102*, 103302.

(5) Vasilopoulou, M.; Georgiadou, D. G.; Soultati, A.; Boukos, N.; Gardelis, S.; Palilis, L. C.; Fakis, M.; Skoulatakis, G.; Kennou, S.; Botzakaki, M.; Georga, S.; Krontiras, C. A.; Auras, F.; Fattakhova-Rohlfing, D.; Bein, T.; Papadopoulos, T. A.; Davazoglou, D.; Argitis, P. Atomic-Layer-Deposited Aluminum and Zirconium Oxides for Surface Passivation of TiO_2 in High-Efficiency Organic Photovoltaics. *Adv. Energy Mater.* **2014**, *4*, 1400214.

(6) Trost, S.; Zilberberg, K.; Behrendt, A.; Polywka, A.; Görrn, P.; Reckers, P.; Maibach, J.; Mayer, T.; Riedl, T. Overcoming the "Light-Soaking" Issue in Inverted Organic Solar Cells by the Use of Al:ZnO Electron Extraction Layers. *Adv. Energy Mater.* **2013**, *3*, 1437−1444.

(7) Kim, J.; Kim, G.; Choi, Y.; Lee, J.; Heum Park, S.; Lee, K. Light-Soaking Issue in Polymer Solar Cells: Photoinduced Energy Level Alignment at the Sol-Gel Processed Metal Oxide and Indium Tin Oxide Interface. *J. Appl. Phys.* **2012**, *111*, 114511-1−114511-9.

(8) Guerrero, A.; Chambon, S.; Hirsch, L.; Garcia-Belmonte, G. Light-Modulated TiOx Interlayer Dipole and Contact Activation in Organic Solar Cell Cathodes. *Adv. Funct. Mater.* **2014**, *24*, 6234−6240.

(9) Tremolet de Villers, B. J.; MacKenzie, R. C. I.; Jasieniak, J. J.; Treat, N. D.; Chabinyc, M. L. Linking Vertical Bulk-Heterojunction Composition and Transient Photocurrent Dynamics in Organic Solar Cells with Solution-Processed MoOx Contact Layers. *Adv. Energy Mater.* **2014**, *4*, 1301290.

(10) Bulliard, X.; Ihn, S.-G.; Yun, S.; Kim, Y.; Choi, D.; Choi, J.-Y.; Kim, M.; Sim, M.; Park, J.-H.; Choi, W.; Cho, K. Enhanced Performance in Polymer Solar Cells by Surface Energy Control. *Adv. Funct. Mater.* **2010**, *20*, 4381−4387.

(11) Kim, M. G.; Kanatzidis, M. G.; Facchetti, A.; Marks, T. J. Low-Temperature Fabrication of High-Performance Metal Oxide Thin-Film Electronics via Combustion Processing. *Nat. Mater.* **2011**, *10*, 382−388.

(12) Chandra, R. D.; Rao, M.; Zhang, K.; Prabhakar, R. R.; Shi, C.; Zhang, J.; Mhaisalkar, S. G.; Mathews, N. Tuning Electrical Properties in Amorphous Zinc Tin Oxide Thin Films for Solution Processed Electronics. *ACS Appl. Mater. Interfaces* **2013**, *6*, 773−777.

(13) Häming, M.; Issanin, A.; Walker, D.; Von Seggern, H.; Jägermann, W.; Bonrad, K. Interrelation between Chemical, Electronic, and Charge Transport Properties of Solution-Processed Indium-Zinc Oxide Semiconductor Thin Films. *J. Phys. Chem. C* **2014**, *118*, 12826−12836.

(14) Choi, C. G.; Seo, S. J.; Bae, B. S. Solution-Processed Indium-Zinc Oxide Transparent Thin-Film Transistors. *Electrochem. Solid-State Lett.* **2008**, *11*, H7−H9.

(15) Lee, D. H.; Han, S. Y.; Herman, G. S.; Chang, C. H. Inkjet Printed High-Mobility Indium Zinc Tin Oxide Thin Film Transistors. *J. Mater. Chem.* **2009**, *19*, 3135−3137.

(16) Jeong, S.; Ha, Y. G.; Moon, J.; Facchetti, A.; Marks, T. J. Role of Gallium Doping in Dramatically Lowering Amorphous-Oxide Processing Temperatures for Solution-Derived Indium Zinc Oxide Thin-Film Transistors. *Adv. Mater.* **2010**, *22*, 1346−1350.

(17) Kim, Y. H.; Heo, J. S.; Kim, T. H.; Park, S.; Yoon, M. H.; Kim, J.; Oh, M. S.; Yi, G. R.; Noh, Y. Y.; Park, S. K. Flexible Metal-Oxide Devices Made by Room-Temperature Photochemical Activation of Sol-Gel Films. *Nature* **2012**, *489*, 128−132.

(18) Lim, W.; Kim, S.; Wang, Y. L.; Lee, J. W.; Norton, D. P.; Pearton, S. J.; Ren, F.; Kravchenko, I. I. High-Performance Indium Gallium Zinc Oxide Transparent Thin-Film Transistors Fabricated by Radio-Frequency Sputtering. *J. Electrochem. Soc.* **2008**, *155*, H383−H385.

(19) Oo, T. Z.; Devi Chandra, R.; Yantara, N.; Prabhakar, R. R.; Wong, L. H.; Mathews, N.; Mhaisalkar, S. G. Zinc Tin Oxide (ZTO) Electron Transporting Buffer Layer in Inverted Organic Solar Cell. *Org. Electron.* **2012**, *13*, 870−874.

(20) Kyaw, A. K. K.; Wang, Y.; Zhao, D. W.; Huang, Z. H.; Zeng, X. T.; Sun, X. W. The Properties of Sol-gel Processed Indium-Doped Zinc Oxide Semiconductor Film and Its Application in Organic Solar Cells. *Phys. Status Solidi A* **2011**, *208*, 2635−2642.

(21) Thambidurai, M.; Kim, J. Y.; Kang, C. M.; Muthukumarasamy, N.; Song, H. J.; Song, J.; Ko, Y.; Velauthapillai, D.; Lee, C. Enhanced Photovoltaic Performance of Inverted Organic Solar Cells with In-Doped ZnO as an Electron Extraction Layer. *Renewable Energy* **2014**, *66*, 433−442.

(22) Chiam, S. Y.; Liu, Z. Q.; Pan, J. S.; Manippady, K. K.; Wong, L. M.; Chim, W. K. Effects of Electric Field in Band Alignment Measurements Using Photoelectron Spectroscopy. *Surf. Interface Anal.* **2012**, *44*, 1091−1095.

(23) Jiang, Q.; Lu, J.; Cheng, J.; Li, X.; Sun, R.; Feng, L.; Dai, W.; Yan, W.; Ye, Z. Combustion-Process Derived Comparable Performances of Zn-(In:Sn)-O Thin-Film Transistors with a Complete Miscibility. *Appl. Phys. Lett.* **2014**, *105*, 132105.

(24) Nadaud, N.; Lequeux, N.; Nanot, M.; Jové, J.; Roisnel, T. Structural Studies of Tin-Doped Indium Oxide (ITO) and $In_4Sn_3O_{12}$. *J. Solid State Chem.* **1998**, *135*, 140−148.

(25) Kang, Y. H.; Jeong, S.; Ko, J. M.; Lee, J.-Y.; Choi, Y.; Lee, C.; Cho, S. Y. Two-Component Solution Processing of Oxide Semiconductors for Thin-Film Transistors via Self-Combustion Reaction. *J. Mater. Chem. C* **2014**, *2*, 4247−4256.

(26) Ramamoorthy, K.; Kumar, K.; Chandramohan, R.; Sankaranarayanan, K.; Saravanan, R.; Kityk, I. V.; Ramasamy, P. High Optical Quality IZO ($In_2Zn_2O_5$) Thin Films by PLD − A Novel Development for III−V Opto-Electronic Devices. *Opt. Commun.* **2006**, *262*, 91−96.

(27) Lee, D. H.; Chang, Y. J.; Herman, G. S.; Chang, C. H. A General Route to Printable High-Mobility Transparent Amorphous Oxide Semiconductors. *Adv. Mater.* **2007**, *19*, 843−847.

(28) Kim, M.-G.; Kim, H. S.; Ha, Y.-G.; He, J.; Kanatzidis, M. G.; Facchetti, A.; Marks, T. J. High-Performance Solution-Processed Amorphous Zinc−Indium−Tin Oxide Thin-Film Transistors. *J. Am. Chem. Soc.* **2010**, *132*, 10352−10364.

(29) Pachoumi, O.; Li, C.; Vaynzof, Y.; Banger, K. K.; Sirringhaus, H. Improved Performance and Stability of Inverted Organic Solar Cells with Sol-Gel Processed, Amorphous Mixed Metal Oxide Electron Extraction Layers Comprising Alkaline Earth Metals. *Adv. Energy Mater.* **2013**, *3*, 1428−1436.

DOI: 10.1021/acsami.5b02215
ACS Appl. Mater. Interfaces 2015, 7, 11099−11106

(30) Crispin, X.; Geskin, V.; Crispin, A.; Cornil, J.; Lazzaroni, R.; Salaneck, W. R.; Brédas, J.-L. Characterization of the Interface Diopole at Organic/Metal Interfaces. *J. Am. Chem. Soc.* **2002**, *124*, 8131−8141.
(31) Cowan, S. R.; Schulz, P.; Giordano, A. J.; Garcia, A.; MacLeod, B. A.; Marder, S. R.; Kahn, A.; Ginley, D. S.; Ratcliff, E. L.; Olson, D. C. Chemically Controlled Reversible and Irreversible Extraction Barriers via Stable Interface Modification of Zinc Oxide Electron Collection Layer in Polycarbazole-based Organic Solar Cells. *Adv. Funct. Mater.* **2014**, *24*, 4671−4680.
(32) van Duren, J. K. J.; Yang, X.; Loos, J.; Bulle-Lieuwma, C. W. T.; Sieval, A. B.; Hummelen, J. C.; Janssen, R. A. J. Relating the Morphology of Poly(p-phenylene vinylene)/Methanofullerene Blends to Solar-Cell Performance. *Adv. Funct. Mater.* **2004**, *14*, 425−434.

DOI: 10.1021/acsami.5b02215
ACS Appl. Mater. Interfaces 2015, 7, 11099−11106